A Spectral-Domain Analysis of Periodically Nonuniform Microstrip Lines

FRANZ J. GLANDORF AND INGO WOLFF, SENIOR MEMBER, IEEE

Abstract — **Periodically nonuniform microstrip lines are analyzed on the basis of a numerical field calculation. Floquet's theorem is used to express all field quantities in terms of their spatial harmonics, so that the problem can be treated similarly to the uniform microstrip line. The boundary-value problem for the microstrip line in an enclosure is formulated in a rigorous way and then solved using Galerkin's method in the Fourier-transform domain. Numerical and experimental results are presented for a sinusoidal and a zigzag-shaped microstrip line.**

I. Introduction

THIS PAPER describes investigations on microstrip lines with strip widths which change periodically in the z-coordinate direction (the direction of wave propagation). Such lines from now on shall be called periodically nonuniform microstrip lines. Fig. 1 shows three examples of such periodically nonuniform microstrip lines.

Like all waveguides with cross sections which vary periodically in the direction of wave propagation, the periodically nonuniform microstrip lines have the following electrical properties (e.g., [1]).

1) Waves propagating on such lines have phase velocities much smaller than the propagation velocity of light in an equivalent medium; they therefore can be used as slow-wave structures.

2) The transmission properties of periodic waveguides are characterized by passbands and stopbands. These properties can be used to realize filtering structures.

The electromagnetic field of the uniform microstrip line is a hybrid mode; i.e., the magnetic field and the electric field have longitudinal field components. This hybrid-mode character of the field makes the exact analysis of the microstrip line difficult, and the numerical methods normally used are complicated (e.g., [2]–[4]). The field-theoretical analysis of nonuniform microstrip lines is even more complicated. Therefore, up to now most of the theories described in the literature are based on simplifying assumptions, e.g., on the assumption of a TEM-mode character of the electromagnetic field [5]–[7], or on a waveguide model for simplifying the calculations [7], [8].

Several papers have been published which describe experimental investigations on periodically nonuniform microstrip lines [10]–[12]. Additionally, there are some descriptions of calculation methods which use simplifying assumptions. One method [16] which does not use restrictive assumptions has also been applied to periodically nonuniform microstrip lines.

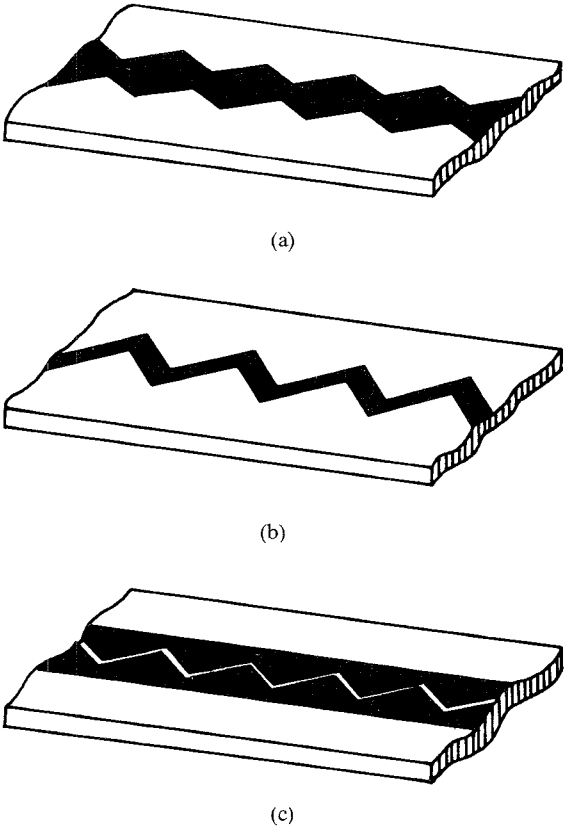

Fig. 1. Three examples for periodically nonuniform microstrip lines.

In this paper, the special problem of periodically nonuniform microstrip lines shall be investigated on the basis of a numerical calculation of the electromagnetic field distribution on the line in the spectral domain. This method is evaluated for some examples and the theoretical results are compared to measurements with frequency dependence. Additionally, the frequency-dependent voltage and current distributions on the line are investigated and described.

Manuscript received September 25, 1985; revised September 23, 1986.

F. J. Glandorf was with the Department of Electrical Engineering, Duisburg University. He is now with ANT Nachrichtentechnik, Backnang, West Germany.

I. Wolff is with the Department of Electrical Engineering, Duisburg University, Duisburg, West Germany.

IEEE Log Number 8612569.

II. Analysis on the Basis of the Electromagnetic Field Theory

A covered, periodically nonuniform microstrip line of the type shown in Fig. 2(a) is considered. All geometrical parameters and material parameters are defined in Fig. 2.

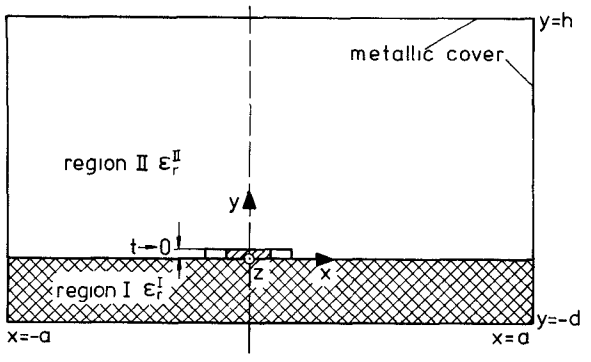

(a)

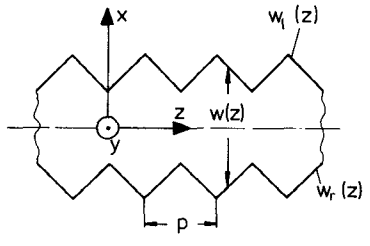

(b)

Fig. 2. (a) Cross section of the periodically nonuniform microstripline considered and (b) an example for a possible strip geometry.

Fig. 2(b) shows an example of the top metallization, a zigzag-shaped strip being chosen in this case. The metallization thickness is assumed to be zero. The periodically varying width of the strip is defined by the two periodic functions $w_l(z)$ (left side) and $w_r(z)$ (right side) as a function of the z coordinate. The width of the strip at the coordinate z is therefore $w(z) = w_l(z) - w_r(z)$. The periodicity (length of one period) of the line is p.

The theory for the periodically nonuniform microstrip line described here is based principally on the method of Jansen [3], [17], [18], which was developed for the uniform microstrip line. This method consequently considers the hybrid-mode character of the electromagnetic field. It has good convergence behavior, has few final equations, and needs relatively short computer time.

Jansen's method for the covered microstrip line [18] describes the electromagnetic fields in regions I and II (Fig. 2) using two potential functions for each region, $\vec{\phi}^{I,II}(x, y, z)$ and $\vec{\Psi}^{I,II}(x, y, z)$, which satisfy the wave equation. Using these potential functions, the electromagnetic fields in the field regions I and II can be calculated with the help of Maxwell's equations.

A wave propagation in the z direction is described by the potential functions as follows:

$$\phi^i(x, y, z) = \phi_p^i(x, y, z)e^{-j\beta z}$$

$$\Psi^i(x, y, z) = \Psi_p^i(x, y, z)e^{-j\beta z}, \qquad i = I, II. \tag{1}$$

In contrast to the case of the uniform microstrip line, in the case of the periodically nonuniform microstrip line the functions $\phi_p^i(x, y, z)$ and $\Psi_p^i(x, y, z)$ are still periodic functions of the coordinate z (Floquet's theorem [19]). This means that the potential functions can be developed into Fourier series with respect to the z coordinate:

$$\phi_p^i(x, y, z) = \sum_{k=-\infty}^{k=+\infty} \varphi_k^i(x, y)e^{j(2\pi k/p)z}$$

$$\Psi_p^i(x, y, z) = \sum_{k=-\infty}^{k=+\infty} \psi_k^i(x, y)e^{j(2\pi k/p)z}. \tag{2}$$

Therefore, for the total potential functions $\phi^i(x, y, z)$ and $\Psi^i(x, y, z)$, the following equations are valid:

$$\phi^i(x, y, z) = \sum_{k=-\infty}^{k=+\infty} \varphi_k^i(x, y)e^{j\beta_k z}$$

$$\Psi^i(x, y, z) = \sum_{k=-\infty}^{k=+\infty} \psi_k^i(x, y)e^{j\beta_k z},$$

$$\text{with } \beta_k = \frac{2\pi k}{p} - \beta. \tag{3}$$

As a consequence, the electromagnetic field forms an infinite spectrum of electromagnetic waves with different phase constants β_k. The single spectral components shall be called space harmonics.

For brevity and clearness, only lines symmetric with respect to the z axis are considered, and only waves with an even y component of the electric field strength with x-coordinate dependence shall be discussed here. Of course, the theory may also be applied to all other cases if it is required, but the assumption made here is

$$w_r(z) = -w_l(z)$$

$$E_y(x, y, z) = E_y(-x, y, z). \tag{4}$$

This assumption means that the potential functions φ_k^i must be odd with respect to the x coordinate while the potential functions Ψ_k^i must be even with respect to the x coordinate; they must satisfy the boundary conditions at the metallic cover and on the ground plane, as in the case of the uniform microstrip line.

The space harmonics of the potential functions $\Phi^{I,II}$ and $\Psi^{I,II}$ can be developed into a series of harmonic functions in such a way that each space harmonic independently satisfies the boundary conditions and the wave equation:

$$\varphi_k^i(x, y) = \sum_{n=1}^{\infty} a_{nk}^i \cos\left(k_{ynk}^i\{y + y^i\}\right)\sin(k_{xn}x)$$

$$\psi_k^i(x, y) = \sum_{n=1}^{\infty} b_{nk}^i \sin\left(k_{ynk}^i\{y + y^i\}\right)\cos(k_{xn}x) \tag{5}$$

where $i = I, II$, $y^I = d$, $y^{II} = -h$, $k_{xn} = (n - 0.5)\pi/a$, and $k_{ynk}^i = k_i^2 - k_{xn}^2 - \beta_k^2$.

The coefficients a_{nk}^i and b_{nk}^i now have to be determined so that on the surface of the dielectric substrate material the boundary conditions for the tangential electric and magnetic field strength are fulfilled, i.e.,

$$(\vec{E}^I - \vec{E}^{II}) \times \vec{e}_y = \vec{0}$$

$$(\vec{H}^I - \vec{H}^{II}) \times \vec{e}_y = \vec{J}(x, z). \tag{6}$$

$\vec{J}(x, z)$, the surface current density in the metallic strip, is a function of the coordinate x as well as the coordinate z.

The surface current density of the periodically nonuniform microstrip line consists of an infinite spectrum of space harmonics also; therefore, as in the case of the other field components, it may also be developed into a Fourier series with respect to the z coordinate. Additionally, it must be possible to develop this quantity into a Fourier series with respect to the x coordinate with a periodicity of $4a$, because the width of the metallic cover (which is half the periodicity) is chosen to be $2a$ (Fig. 2(a)). The x component and the z component are even functions of x for the even modes, which are the only ones considered here (see above). Therefore, the two-dimensional Fourier series expansion of $\vec{J}$ is

$$\vec{J} = \sum_{k=-\infty}^{k=+\infty} \sum_{n=1}^{\infty} \overleftrightarrow{S}_n \vec{J}_{nk} e^{j\beta_k z} \tag{7}$$

where $\overleftrightarrow{S}_n$ is a matrix:

$$\overleftrightarrow{S}_n = \begin{pmatrix} \sin(k_{xn}x) & 0 \\ 0 & \cos(k_{xn}x) \end{pmatrix}$$

and

$$\vec{J}_{nk} = \begin{pmatrix} J_{xnk} \\ J_{znk} \end{pmatrix}.$$

If the electromagnetic field is calculated using the potential functions given in (2) or (5), respectively, and if in addition the boundary conditions are introduced into these equations, the unknown coefficients a^{I}_{nk}, a^{II}_{nk}, b^{I}_{nk}, and b^{II}_{nk} can be determined as functions of the Fourier series coefficients $\vec{J}_{nk}$ of the surface current density by a comparison of the coefficients of the resulting systems of equations.

The total electromagnetic field of the periodically nonuniform microstrip line therefore can be described by the (up to now) unknown Fourier coefficients $\vec{J}_{nk}$ of the surface current density. Especially, for the electrical field strength which is tangential to the plane $y = 0$, the following equation results:

$$\begin{aligned} \vec{E}_t &= \vec{E}^{\mathrm{I}}|_{y=0} \times \vec{e}_y = \vec{E}^{\mathrm{II}}|_{y=0} \times \vec{e}_y \\ &= \sum_{k=-\infty}^{k=+\infty} \sum_{n=1}^{\infty} \overleftrightarrow{S}_n \overleftrightarrow{\Gamma}_{nk} \vec{J}_{nk} e^{j\beta_k z} \end{aligned} \tag{8a}$$

with

$$\overleftrightarrow{\Gamma}_{nk} = \begin{pmatrix} j\Gamma_{xxnk} & \Gamma_{xznk} \\ -\Gamma_{xznk} & j\Gamma_{zznk} \end{pmatrix} \tag{8b}$$

and

$$\Gamma_{xxnk} = -\left[\frac{\beta_k^2}{\Pi_{nk}} + \frac{k_{xn}^2}{\theta_{nk}}\right]$$

$$\Gamma_{xznk} = \beta_k k_{xn}\left[\frac{1}{\theta_{nk}} - \frac{1}{\Pi_{nk}}\right]$$

$$\Gamma_{zznk} = -\left[\frac{k_{xn}^2}{\Pi_{nk}} + \frac{\beta_k^2}{\theta_{nk}}\right]$$

$$\Pi_{nk} = \frac{k_{xn}^2 + \beta_k^2}{\omega\mu_0}\left[\frac{k_{yn}^{\mathrm{I}2}}{T^{\mathrm{I}}_{nk}} + \frac{k_{yn}^{\mathrm{II}2}}{T^{\mathrm{II}}_{nk}}\right]$$

and

$$\theta_{nk} = k_0^2 \frac{(k_{xn}^2 + \beta_k^2)}{\omega\mu_0}\left[\frac{\epsilon_r^{\mathrm{I}}}{T^{\mathrm{I}}_{nk}} + \frac{\epsilon_r^{\mathrm{II}}}{T^{\mathrm{II}}_{nk}}\right] \tag{8c}$$

where

$$\begin{aligned} T^{\mathrm{I}}_{nk} &= k^{\mathrm{I}}_{ynk} \tan\left(k^{\mathrm{I}}_{ynk} d\right) \\ T^{\mathrm{II}}_{nk} &= k^{\mathrm{II}}_{ynk} \tan\left(k^{\mathrm{II}}_{ynk} h\right). \end{aligned} \tag{8d}$$

III. The Solution of the Boundary-Value Problem Using Galerkin's Method

Equation (8) describes the electric field which is tangential to the boundary between the dielectric substrate material and the air region by means of a two-dimensional Fourier series with respect to the surface current density on the boundary. On the metallic strip (which is assumed to be of infinite conductivity) the tangential electric field strength must vanish.

To find a solution of this eigenvalue problem, the surface current density and the phase constant have to be determined so that the condition $\vec{E}_t \equiv 0$ for $w_r(z) \leqslant x \leqslant w_l(z)$ and all values of z is satisfied.

This problem shall be solved using Galerkin's method; for this purpose, the surface current density is expanded into a series using a functional system which still has to be chosen appropriately:

$$\vec{J} = \sum_{\iota=1}^{\infty} U_\iota(z)\, \vec{X}_\iota(x,z)\, e^{j\beta_k z} \tag{9}$$

with

$$\vec{X}_\iota = \begin{pmatrix} X_{\iota x} \\ X_{\iota z} \end{pmatrix} \quad \text{and} \quad \vec{X}_\iota \equiv 0 \quad \text{for} \begin{cases} -a \leqslant x \leqslant w_r(z) \\ w_l(z) \leqslant x \leqslant a. \end{cases}$$

In (9), the vector function $\vec{X}_\iota$ is used to describe the x dependence of the surface current density for values $z =$ const. Because these functions are identically zero outside the metallic strip and because of the z-dependent strip width, these functions must be z dependent also. The dependence of the surface current density on the z coordinate which results from the electromagnetic field will be described by the functions $U_\iota(z)$; they are periodic functions having periodicity p. Their Fourier series expansion is given by

$$U_\iota(z) = \sum_{l=-\infty}^{+\infty} u_{\iota l} e^{j(2\pi l/p)z}. \tag{10}$$

With this, together with (9), the Fourier coefficients describing the surface current density in (7) can be written as

$$\vec{J}_{nk} = \sum_{\iota=1}^{\infty} \sum_{l=-\infty}^{\infty} u_{\iota l} \vec{X}_{nk\iota l} \tag{11}$$

with

$$\vec{X}_{nk\iota l} = \frac{1}{4ap} \int_{z_0}^{z_0+p} \int_{w_r(z)}^{w_l(z)} \overleftrightarrow{S}_n \vec{X}_\iota e^{j(2\pi/p)(l-k)z}\, dx\, dz.$$

If these coefficients are introduced into (8), the tangential

electric field strength is

$$\vec{E}_t = \sum_{n=1}^{\infty} \sum_{k=-\infty}^{+\infty} \vec{S}_{nk} \vec{\Gamma}_{nk} \left(\sum_{i=1}^{\infty} \sum_{l=-\infty}^{+\infty} u_{il} \vec{X}_{nkil} \right) e^{j\beta_k z}$$

$$\vec{E}_t = \sum_{i=1}^{\infty} \sum_{l=-\infty}^{+\infty} u_{il} \left(\sum_{n=1}^{\infty} \sum_{k=-\infty}^{+\infty} \vec{S}_{nk} \vec{\Gamma}_{nk} \vec{X}_{nkil} e^{j\beta_k z} \right). \quad (12)$$

To satisfy the condition that the tangential electric field strength vanish on the metallic strip, the moment method in its special form of Galerkin's method [20] is used. This means that the scalar product formed by the tangential electric field strength and by the expansion functions of the surface current density must vanish:

$$\int_{z_0}^{z_0+p} \int_{w_r(z)}^{w_l(z)} \vec{X}_r^{*T}(x,z) \vec{E}_t(x,z) e^{-j\beta_s z} \, dx \, dz = 0 \quad (13)$$

with $r = 1, 2, \cdots, \infty$ and $s = -\infty, \cdots, -1, 0, 1, \cdots, +\infty$.

If the tangential electric field strength given in (12) is introduced into (13) and if in addition the succession of integration and summation is exchanged, the infinite equation system of the following form is derived:

$$\sum_{i=1}^{\infty} \sum_{l=-\infty}^{+\infty} u_{il} \sum_{n=1}^{\infty} \sum_{k=-\infty}^{+\infty} \int_{z_0}^{z_0+p} \int_{w_r(z)}^{w_l(z)} \vec{X}_r^{*T} \vec{\Gamma}_{nk} \vec{X}_{nkil} \cdot e^{j(2\pi/p)(k-s)} \, dx \, dz$$

$$= \sum_{i=1}^{\infty} \sum_{l=-\infty}^{+\infty} u_{il} \sum_{n=1}^{\infty} \sum_{k=-\infty}^{\infty} \vec{X}_{nkrs}^{*T} \vec{\Gamma}_{nk} \vec{X}_{nkil}$$

$$= \sum_{i=1}^{\infty} \sum_{l=-\infty}^{+\infty} u_{il} P_{rsil} = 0 \quad (14)$$

for $r = 1, 2, \cdots, \infty$ and $s = -\infty, \cdots, -1, 0, 1, \cdots, +\infty$. Here,

$$P_{rsil} = \sum_{n=1}^{\infty} \sum_{k=-\infty}^{k=+\infty} \vec{X}_{nkrs}^{*T} \vec{\Gamma}_{nk} \vec{X}_{nkil}.$$

For the numerical evaluation, the infinite series are truncated at finite values of the indices. If the maximum values of the indices i and l are $i = I$ and $l = \pm L$, then $(2L+1)I$ unknown coefficients u_{il} have to be determined. If the same truncation for the series with indices r and s is made, the number of equations is equal to the number of unknown coefficients u_{il}.

The highest value of the index k is evaluated from the indices l and s. Only elements of the Fouriers series of the surface current density given in (11) up to the order of M are considered, where M must satisfy the conditions $|l-k| \leqslant M$ and $|s-k| \leqslant M$. The highest value of the index n will be designated N.

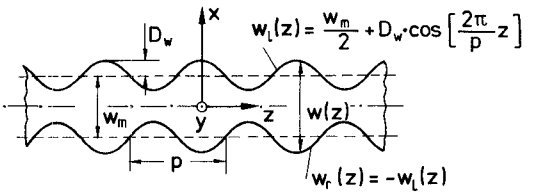

Fig. 3. Strip geometry of a periodically nonuniform microstrip line with sinusoidally variable strip width.

The finite homogeneous equation system has a nontrivial solution only if the determinant of the system matrix is zero. The elements of the system matrix are functions of the geometrical parameters of the microstrip line, the frequency and the phase constants. The zeros of the determinant therefore can be determined either as a function of the wavelength for a given frequency or as a function of the frequency if the wavelength is given. The unknown coefficients u_{il} may then be easily calculated within a constant factor. Using these coefficients, the electrical surface current density in the metallic strip and, therefore, the electromagnetic field in all field regions of the structure (Fig. 2(a)) can be computed.

IV. The Numerical Evaluation

The convergence of the numerical method is heavily influenced by the choice of the expansion functions of the surface current density. Two physical properties must be taken into account when the expansion functions are chosen.

1) It must be borne in mind that the current density cannot have a component perpendicular to the edge of the metallic strip. This condition will be satisfied if all expansion functions $\vec{X}_i(x,z)$ have only components parallel to the curves defined by $w_r(l)$ and $w_l(z)$ (Fig. 3).

2) Additionally, consideration must be given to the fact that the surface current density has a pole at the strip edge (edge condition). Therefore, the expansion functions are chosen so that this pole is approximated fairly well *a priori*.

A system of expansion functions which satisfies these requirements is

$$\vec{X}_i(x,z) = \frac{1}{\sqrt{1-\left(\frac{2x}{w(z)}\right)^2}} \cdot \begin{pmatrix} \cos(\alpha(x,z)) & \sin(\alpha(x,z)) \\ -\sin(\alpha(x,z)) & \cos(\alpha(x,z)) \end{pmatrix} \begin{pmatrix} f_{xi}(x,z) \\ f_{zi}(x,z) \end{pmatrix}$$

with

$$f_{xi}(x,z) = \begin{cases} \sin\left(\frac{2i\pi x}{w(z)}\right) & \text{for } 1 \leqslant i < I_z \text{ and } w_r < x < w_l \\ 0 & \text{for } I_z \leqslant i \leqslant I \text{ or } x > w_l(x) \quad x < w_r(x) \end{cases}$$

$$f_{zi}(x,z) = \begin{cases} \cos\left(\frac{2(i-I_z)\pi x}{w(z)}\right) & \text{for } I_z \leqslant i \leqslant I \text{ and } w_r < x < w_l \\ 0 & \text{for } 1 \leqslant i < I_z \text{ or } x > w_l(x) \quad x < w_r(x) \end{cases}$$

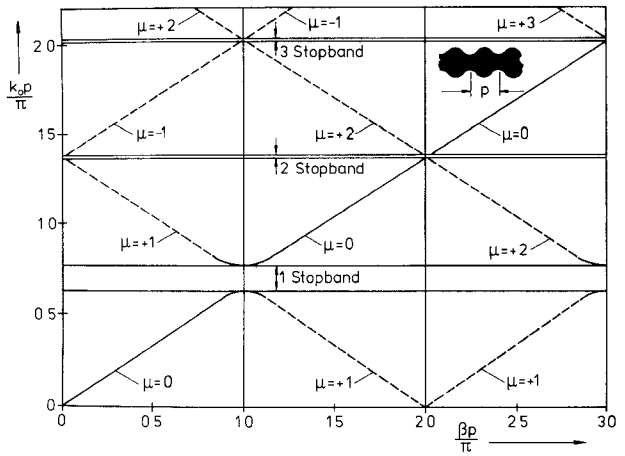

Fig. 4. Brillouin diagram of the fundamental mode on a periodically nonuniform microstrip line with sinusoidally variable strip width.

and

$$\alpha(x,z)=\frac{2\arctan\left(\dfrac{dw_l(z)}{dz}\right)}{w(z)}\cdot x. \tag{15}$$

The integrals defining the Fourier coefficients in (11) can be evaluated in closed form with respect to the x coordinate if these expansion functions are used. They must be integrated numerically with respect to the z coordinate.

As an example, a periodically nonuniform microstrip line with sinusoidally varying strip width (Fig. 3) shall be discussed. The system of equations (14) has been derived for the covered microstrip line shown in Fig. 2; therefore, not only does (14) contain the solutions for the electromagnetic field modes which are propagating in the microstrip structure; in addition, waveguide modes inside the metallic cover may be found. Only the microstrip mode which in the case of a decreasing amplitude D_w of the width function (Fig. 3) converges into the quasi-TEM mode of the uniform microstrip line shall be of interest here. In the following, this mode will be called the fundamental mode of the periodically nonuniform microstrip line.

Fig. 4 shows (in the manner usually applied in the case of periodically nonuniform lines) the frequency-dependent transmission properties of the microstrip line given in Fig. 3 in the $\beta-k_0$ plane (Brillouin diagram). The transmission properties are given by the solid lines in this diagram. As can be seen from the figure, the line has the typical transmission properties of periodic lines characterized by stopbands and passbands.

If a solution of the infinite equation system exists for a frequency f and a phase constant β, the equation system also has a solution for the frequency f and the phase constant $\beta'=\beta+2\pi\mu/p$, with $\mu=\pm1,\pm2,\pm3,\cdots$ (Floquet's theorem). These different solutions are classified as solutions of order μ. In Fig. 4, the solid lines represent the solution of order zero. The solutions of order $\mu\neq0$ can be transformed into solutions of the order $\mu=0$ if the indices l and k (14) are replaced by $l'=l-\mu$ and $k'=k-\mu$. The solutions of order $\mu\neq0$ therefore describe the same mode as the solution of order $\mu=0$.

Additionally, since a wave in the negative z direction must be a solution of the eigenvalue problem, the equations may also be solved for the frequency f and the phase constant $\beta'=-\beta$. Solutions of the order $\mu\neq0$ exist for waves which propagate in the negative z direction as well as in the positive z direction.

In Fig. 4, solutions of order $\mu\neq0$ are shown as dashed lines. The curves with a positive slope characterize the wave modes propagating in the positive z direction, whereas the curves with a negative slope describe waves which propagate in the negative z direction. The curves in Fig. 4 which represent solutions of order $\mu\neq0$ also can be interpreted as the dispersion curves of the space-harmonic partial fields of the fundamental mode.

V. The Convergence of the Numerical Method

The convergence behavior of the numerical method shall be discussed for the example of a periodically inhomogeneous microstrip line with sinusoidally varying strip width. The substrate material used is polyguide material ($\epsilon_r=2.32$) with a thickness of $h=1.56$ mm. The geometrical dimensions of the metallic strip structure (as shown in Fig. 3) are: $W_m=6$ mm, $D_w=1$ mm, and $p=10$ mm.

The stability of the calculated effective dielectric constant $\epsilon_{reff}=(\beta/k_0)^2$ in relation to the different cutoff indices has been taken as a criterion for the convergence of the numerical method. The effective dielectric constant ϵ_{reff} is dependent on the chosen number of expansion functions as well as on the number of Fourier coefficients of the surface current density in the z direction. Additionally, the computation results are influenced by the accuracy with which the expansion functions are described in the spectral domain. This means that the number of coefficients of the two-dimensional Fourier series expansion of the field quantities influences the result. Furthermore, the computations show that the convergence is also frequency dependent.

The relative error of the computed values ϵ_{reff} at a frequency of 1 GHz ($\lambda\approx20p$) is shown in Fig. 5 for a constant number of expansion functions ($I=10$ and $I_z=5$) and a constant number of Fourier coefficients of the surface current density ($L=6$) in relation to the cut-off indices N and M of the two-dimensional Fourier series. As a reference for calculating the relative error, the value of ϵ_{reff} for $I=10$, $I_z=5$, $L=6$, $M=21$, and $N=135$ is chosen. The cutoff index N in Fig. 5 is described by $F=N\cdot W_{\min}/(4I_z a)$. For $F=1.5$ or $N=68$, respectively, $M=11$ and the relative error is smaller than 0.3 percent.

In Fig. 6, the same relative error is shown for a frequency of 5 GHz ($\lambda\approx4p$). It can be seen that the convergence is much better in this case. The relative error is now already smaller than 0.03 percent for $F=0.5$ or $N=23$, respectively, and $M=9$. For satisfactory accuracy of the transformation of the expansion functions into the spectral domain, at least $M\geqslant2D_wN/a$ Fourier coefficients of the Fourier series with respect to the z coordinate have to be

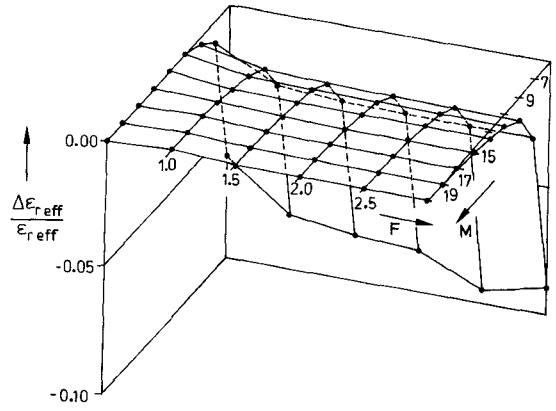

Fig. 5. The convergence of the relative effective dielectric constant at low frequencies ($f=1$ GHz, $\lambda \approx 20p$) for a constant number of expansion functions ($I=10$, $I_z=5$) and a constant number of Fourier coefficients ($L=6$) with cutoff indices N and M of the Fourier series expansion in the spectral domain. See text for the geometry of the line.

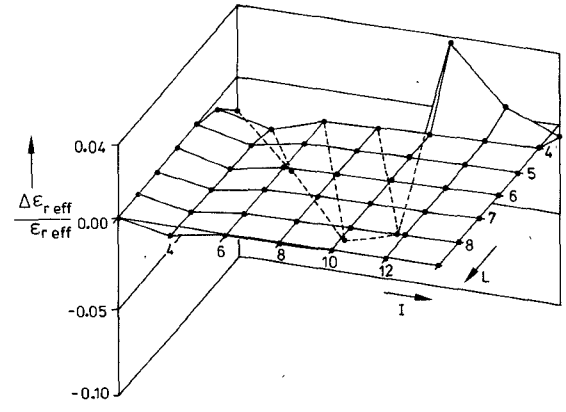

Fig. 7. The convergence of the relative effective dielectric constant at low frequencies ($f=1$ GHz, $\lambda \approx 20p$) for a constant number of Fourier coefficients in the spectral domain ($F=1.7$, $M=17$) in relation to the number I of expansion functions ($I_z=I/2$) and the number L of Fourier coefficients for the surface current density. Line geometry: see text.

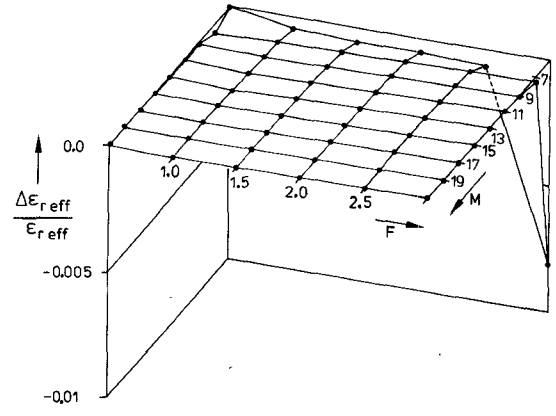

Fig. 6. The convergence of the relative effective dielectric constant at $f=5$ GHz ($\lambda \approx 4p$) and for the conditions given in Fig. 5.

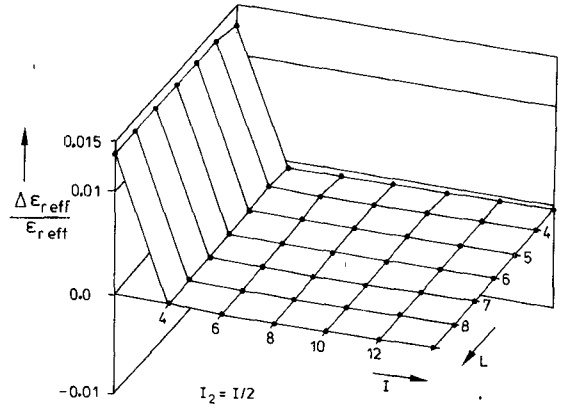

Fig. 8. The convergence of the relative effective dielectric constant at $f=5$ GHz ($\lambda \approx 4p$) under the conditions given in Fig. 7.

considered. This is also the case for investigations on other line geometries.

In Fig. 7, the relative error of the computed effective dielectric constant ϵ_{reff} at a frequency $f=1$ GHz is shown in relation to the chosen number of expansion functions I and $I_z=I/2$ and the number of Fourier coefficients L of the surface current density, while the numbers of Fourier coefficients in the spectral domain are kept constant ($F=1.7$, $M=17$). As a reference in this case, the value of ϵ_{reff} for $F=1.7$, $M=17$, $I=14$, $I_z=7$, and $L=9$ is used. For $L=5$, $I=10$, and $I_z=5$, the relative error is smaller than 0.1 percent.

Fig. 8 again shows the same relative error as described above, but for the frequency $f=5$ GHz ($\lambda \approx 4p$). Again, in this case a better convergence of the method can be recognized than for the lower frequency case. For $I=4$, $I_z=2$, and $L=4$, the relative error already is smaller than 0.02 percent.

The improvement of the convergence with increasing frequency can be explained easily. For low frequencies, one wavelength is equal to several periodic lengths p of the line while for higher frequencies the periodic length is equal to or smaller than the wavelength of the wave on the line. This means that the error per wavelength which results from the final cutoff of the series expansions is larger for low frequencies and smaller for high frequencies.

VI. Numerical and Experimental Results

In this section, some numerical and experimental results for a periodically nonuniform microstrip line with a zigzag geometry (Fig. 9) shall be presented and discussed.

In Fig. 10, the dependence of the computed and measured effective dielectric constant $\epsilon_{reff}=(\beta/k_0)^2$ on the frequency is shown in the frequency range from 1 GHz to 15 GHz. The results for two lines with different values D_w (Fig. 9) of the edge function are presented. The substrate material which was used was Polyguide with a dielectric constant $\epsilon_r=2.32$ and a height $d=1.56$ mm. The amplitude coefficients are $D_w=0.8$ mm and $D_w=1.2$ mm, respectively.

In Fig. 10, the stopbands are shown as shaded areas. For frequencies just below the stopbands, the effective dielectric constant ϵ_{reff} increases but remains finite. For frequencies above the stopbands, the effective dielectric constant is small but is again finite and positive. Additionally, Fig. 10 shows the measured results of the effective dielectric constant in the case of the two lines. The agreement between theory and measurement is good.

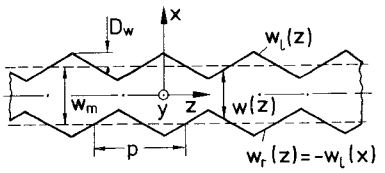

Fig. 9. Strip geometry of a periodically nonuniform microstrip line with a zigzag structure.

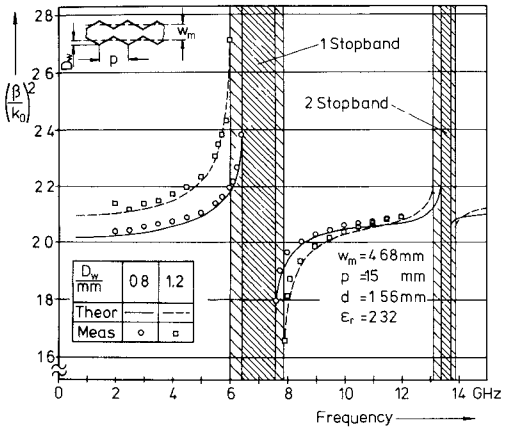

Fig. 10. The effective dielectric constant $\epsilon_{reff} = (\beta/k_0)^2$ of the microstrip line shown in Fig. 9 and the parameters given in the figure.

The fundamental mode of the uniform microstrip line is, at least at low frequencies, quasi-TEM, so that the scalar quantities voltage and current can be defined for these lines under the assumptions made. The same is true for the periodically nonuniform microstrip line. Because the electromagnetic field is periodically dependent on the z coordinate, voltage and current on the line must be periodic functions of the z-coordinate also. The voltage definition which is used here is

$$U(z) = \int_0^{-d} - E_y(x=0, z)\, e^{j\beta z}\, dy. \tag{16}$$

The integral function of the z component of the surface current density over the strip width w at the coordinate z is defined as the strip current:

$$I(z) = \int_{w_r(z)}^{w_l(z)} J_z(x, z)\, e^{j\beta z}\, dx. \tag{17}$$

The voltage $U(z)$ and the current $I(z)$ are normalized to the voltage U_0 and the current I_0 which are, respectively, the voltage and the current of a wave propagating the same power on a uniform microstrip line of width W_m (Fig. 9).

In Fig. 11, the absolute value of the normalized voltage $U(z)/U_0$ is shown for different values $\beta_N = \beta_p/\pi$ between 0.1 and 0.95, i.e., for frequencies below the first stopband.

For $\beta_N = 0.1$, or $\lambda = 20p$, the voltage $|U(z)|$ along the line is constant and equivalent to the voltage of the uniform microstrip line of width W_m if the power transported on both lines is identical. With increasing values of β_N, the voltage increases at the points of broad strip width ($z = 0, \pm p, \pm 2p, \cdots$) whereas it decreases at the points of small strip width ($z = \pm p/2, \pm 3p/2, \cdots$). Therefore, if the frequency approaches the lower limit of the stopband, the planes $z = 0, \pm p, \pm 2p, \cdots$ become magnetic walls,

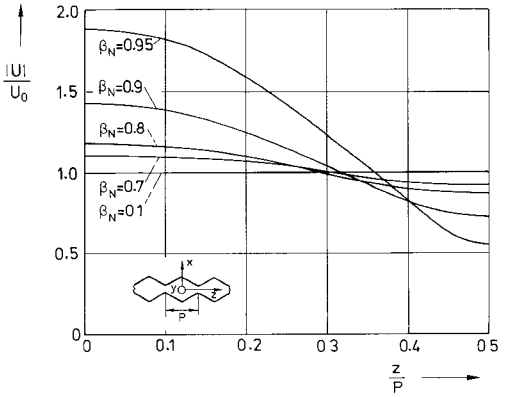

Fig. 11. The normalized absolute value of the voltage on the microstrip line shown in Fig. 9 for different values of β_N in relation to the z coordinate and for a frequency below the first stopband. Geometry parameters: see Fig. 10.

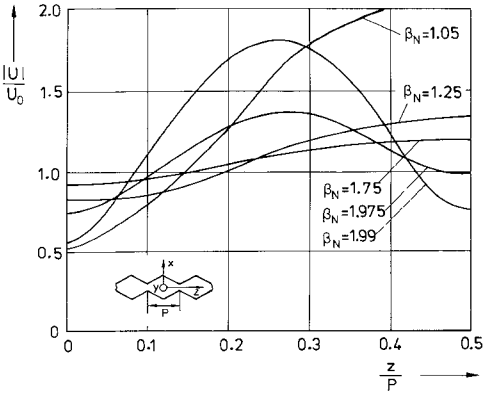

Fig. 12. The normalized absolute value of the voltage on the microstrip line shown in Fig. 9 for different values of β_N in relation to the z coordinate and for a frequency between the first and second stopbands. Geometry parameters: see Fig. 10.

whereas electric walls can be found in the planes $z = \pm p/2, \pm 3p/2, \cdots$ at this frequency.

In Fig. 12, the normalized voltage $|U(z)|/U_0$ is shown for values of β_N between 1.05 and 1.99, i.e., for frequencies between the first and the second stopband. If the frequency approaches the upper limit of the first stopband, the voltage becomes small at $z = 0, \pm p, \pm 2p, \cdots$, i.e., at the points of large strip width, whereas it takes a maximum value at $z = \pm p/2, \pm 3p/2, \cdots$, i.e., at points where the strip width is small. This means that at the upper frequency limit of the first stopband electric walls are positioned at $z = 0, \pm p, \pm 2p, \cdots$, whereas magnetic walls can be found at $z = \pm p/2, \pm 3p/2, \cdots$. The positions of the electric walls and the magnetic walls are therefore exchanged considering the lower and the upper frequency limits of the first stopband.

Additionally, Fig. 12 shows that at the lower frequency limit of the second stopband an electric wall is positioned at $z = 0, \pm p, \pm 2p, \cdots$ as well as at $z = \pm p/2, \pm 3p/2, \cdots$, whereas the planes $z = \pm p/4, \pm 3p/4, \pm 5p/4, \cdots$ contain magnetic walls.

In Figs. 13 and 14, the normalized absolute value $|I(z)|/I_0$ is shown for the same values of β_N. The described position of the electric and the magnetic walls can also be found in these figures.

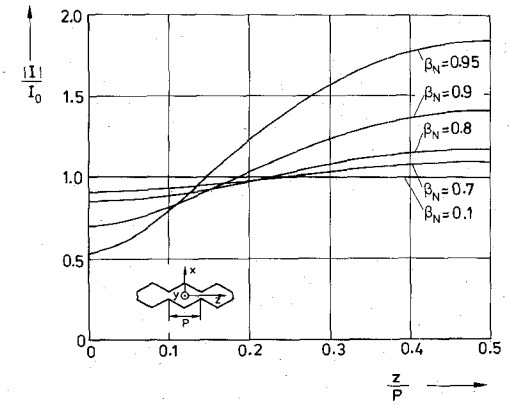

Fig. 13. The normalized absolute value of the current on the microstrip line shown in Fig. 9 for different values of β_N in relation to the z coordinate and for a frequency below the first stopband. Geometry parameters: see Fig. 10.

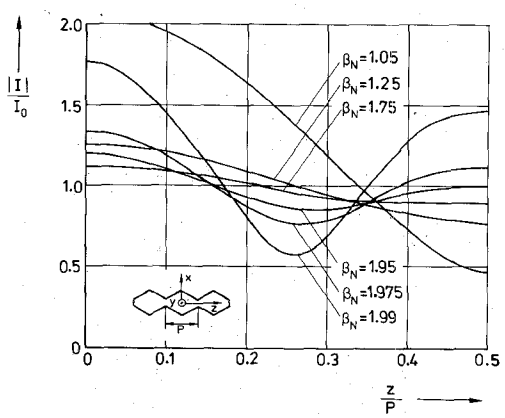

Fig. 14. The normalized absolute value of the current in the microstrip line shown in Fig. 9 for different values of β_N in relation to the z coordinate and for a frequency between the first and the second stopbands. Geometry parameters: see Fig. 10.

VII. Conclusions

A method has been presented for the analysis of periodically nonuniform microstrip lines using the spectral domain technique, and which in contrast to other methods published earlier is rigorous. The method requires considerable numerical effort, but the results are in good agreement with measurements over a wide frequency range.

References

[1] A. W. Lires, G. R. Wicoll, and A. M. Woodward, "Some properties of waveguides with periodic structures," *Proc. Inst. Elec. Eng.*, vol. 97, pt. III, pp. 263–276, July 1950.

[2] T. Itoh and R. Mittra, "Spectral domain approach for calculating the dispersion characteristics of microstrip lines," *IEEE Trans. Microwave Theory Tech.*, vol. MTT-21, pp. 496–499, July 1973.

[3] R. H. Jansen, "A moment method for covered microstrip structures," *Arch. Elek. Übertragung*, vol. 29, pp. 241–247, 1975.

[4] U. Schulz and R. Pregla, "A new technique for the analysis of the dispersion characteristics of planar waveguides," *Arch. Elek. Übertragung*, vol. 34, pp. 169–173, 1980.

[5] A. M. Khilla, "Computer aided design of an optimum Chebyshev microstrip taper," *Arch. Elek. Übertragung*, vol. 35, pp. 133–135, 1981.

[6] K. N. S. Rao, V. Mahaderan, and S. P. Kosta, "Analysis of straight tapered microstrip transmission lines—ASTMIC. Program description," *IEEE Trans. Microwave Theory Tech.*, vol. MTT-25, pp. 164, 1975.

[7] N. V. Nair and A. K. Mallik, "An analysis of a width-modulated microstrip periodic structure," *IEEE Trans. Microwave Theory Tech.*, vol. MTT-32, pp. 200–204, Feb. 1984.

[8] G. Kompa and R. Mehran, "Planar waveguide model for calculating microstrip components," *Electron. Lett.*, vol. 11, no. 19, pp. 459–460, 1975.

[9] W. Menzel, "Calculation of inhomogeneous microstrip lines," *Electron. Lett.*, vol. 13, no. 7, pp. 183–184, 1977.

[10] A. Podell, "A high directivity microstrip coupler technique," in *IEEE G-MTT Int. Microwave Symp. Dig.* (Newport Beach, CA), pp. 33–36, 1970.

[11] J. L. Taylor and P. D. Prigel, "Wiggly phase shifters and directional couplers for radio-frequency hybrid-microstrip applications," *IEEE Trans. Parts, Mater., Packag.*, vol. PHP-12, no. 4, pp. 317–323, 1976.

[12] F. C. de Ronde, "Wide-band high directivity in MIC proximity couplers by planar means," in *IEEE MTT-S Int. Microwave Symp. Dig.*, (Washington, DC), 1980.

[13] T. Sugiura, "Analysis of distributed–lumped strip transmission lines," *IEEE Trans. Microwave Theory Tech.*, vol. MTT-25, pp. 656–661, 1977.

[14] G. Kowalski, "Microstrip meanderlines," *Arch. Elek. Übertragung*, vol. 29, no. 6, pp. 248–250, 1979.

[15] S. K. Chowdhury and C. Bandyopadhyay, "Propagation of electromagnetic waves through a microstrip transmission line with sinusoidally varying width," *Arch. Elek. Übertragung*, vol. 35, no. 3, pp. 135–137, 1981.

[16] S. B. Worm and R. Pregla, "Hybrid-mode analysis of arbitrarily shaped planar microwave structures by the method of lines," *IEEE Trans. Microwave Theory Tech.*, vol. MTT-32, pp. 191–196, 1984.

[17] R. H. Jansen, "High-speed computation of single and coupled microstrip parameters including dispersion, high-order modes, loss and finite strip thickness," *IEEE Trans. Microwave Theory Tech.*, vol. MTT-26, pp. 75–82, 1978.

[18] R. H. Jansen, "Zur numerischen Berechnung der Eigenfrequenzen und Eigenfunktionen von Mikrostrip-Strukturen beliebiger Kontur," Ph.D. thesis, Technical University Aachen, 1975.

[19] R. E. Collin, *Field Theory of Guided Waves*. New York: McGraw Hill, 1960.

[20] R. F. Harrington, *Field Computation by Moment Methods*. New York: Macmillan, 1968.

Franz J. Glandorf was born in Ostercappeln, West Germany, in 1949. He received the Dipl. Ing. degree in electrical engineering from the Aachen Technical University in 1975, and the Dr. Ing. degree from Duisburg University, West Germany, in 1982.

From 1975 to 1982, he was with the Department of Allgemeine und Theoretische Elektrotechnik at Duisburg University. His main research activities were numerical investigations of planar microwave structures. Since 1982, he has been with ANT Nachrichtentechnik, Backnang, West Germany. He is currently working on passive microwave components, mixers, and oscillators for space applications.

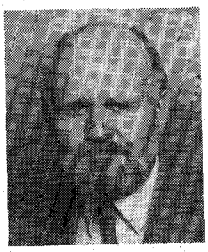

Ingo Wolff (M'75–SM'85) was born in Köslin, Germany, in 1938. He received the Dipl. Ing. degree, the Dr. Ing. degree, and the Habilitation degree from the Technical University of Aachen, West Germany, in 1964, 1967, and 1970, respectively.

He was an Associate Professor for high-frequency techniques for four years at the Technical University of Aachen. Since 1974, he has been a Full Professor for electromagnetic field theory at Duisburg University, Duisburg, West Germany. He has carried out research work on millimeter-wave techniques, ferrite components, computer-aided design of planar microwave components, microwave integrated circuits, and planar microwave antennas. Dr. Wolff is Director of the Research Institute for Microwave and Millimeter-Wave Techniques.